Available online at www.sciencedirect.com

ScienceDirect

Procedia Materials Science 10 (2015) 186 – 194

Procedia Materials Science

www.elsevier.com/locate/procedia

2nd International Conference on Nanomaterials and Technologies (CNT 2014)

Electrospun nanofibers of conducting polyaniline/Al-SnO_2 composites for hydrogen sensing applications

Hemlata J. Sharma*, Dipti V. Jamkar, Subhash B. Kondawar

Department of Physics, Polymer Nanotech Laboratory, Rashtrasant Tukadoji Maharaj Nagpur University, Nagpur – 440033, India.

Abstract

In this paper, we report the synthesis and characterization of composites of polyaniline and aluminum doped tin oxide (Al-SnO_2/PANI) nanofibers for hydrogen gas sensing application. Al-SnO_2/PANI composite nanofibers have been fabricated via electrospinning technique and subsequent calcination procedure. The as-prepared Al-SnO_2/PANI composite nanofibers were investigated for structural characterizations by means of SEM, FTIR, UV-VIS and XRD. SEM revealed the nanofibers with the diameter around 200-300 nm formed a non-woven material with highly porous and agglomerated structure. FTIR and UV-VIS spectra revealed the possible incorporation of Al-SnO_2 in PANI and confirmed the uniform attachment of PANI on the surface of Al-SnO_2 nanostructures. XRD showed peak broadening and the peak positions shift from standard values, indicating presence of aluminum doped tin oxide in nanoparticles form in the polyaniline (PANI) matrix. On exposure to hydrogen gas (1000 ppm), it was found that the nanofibers of Al-SnO_2/PANI composite showed high sensitivity at 48 ^oC with relatively faster response/recovery as compared to pure SnO_2 and Al doped SnO_2 nanofibers.

Peer-review under responsibility of the International Conference on Nanomaterials and Technologies (CNT 2014)

Keywords: Nanofibers; Aluminium Doped Tin Oxide; Polyaniline; Nanocomposites; Electrospinning; Hydrogen Sensing.

*Corresponding Author Tel.: +91-712-2042086 ;
E-mail Address: hemlatasharma208@gmail.com

1. Introduction

Environmental sustainability is a pressing and growing problem due to issues such as climate change, pollution and disturbances associated with biodiversity. A major cause of these environmental threats is pollutants in the atmosphere, Binions and Naik (2013). The gas sensors are highly in demand for detecting, monitoring and controlling the presence of hazardous and poisonous gases in the atmosphere. The fundamental requirements of highly sensitive, selective, stable and fast response gas sensors with economical considerations (multi gas sensor,

Peer-review under responsibility of the International Conference on Nanomaterials and Technologies (CNT 2014)
doi:10.1016/j.mspro.2015.06.040

small size, low production time and low cost) have lead to extensive research and development in gas sensing area. Generally, these sensors are made of metal oxide semiconductors as sensing materials. Tin oxide (SnO_2), compared to the other semiconductor materials based sensor, exhibits better response. Pure tin oxide, SnO_2 is a remarkable n-type semiconductor material having wide band gap (~3.6 eV), and by making use of small quantity of dopant into its matrix, thin films of this material find use in several devices such as flat panel displays, gas sensors for the detection of H_2, NH_3 and NO_2 gases, transparent electrodes, photo sensors, photo catalysts, antistatic coatings and solar cells (Tischner et al. 2008, Tai et al. 2007, Qiu et al. 2011, Patil et al, 2014). By doping, its conductivity increases by several orders of magnitude. However, the sensors incorporating doped tin oxide require an elevated temperature ($\geq$ 200 ˚C) for their optimum operation (Berry and Brunet 2008, Hieu et al. 2008). In addition, the sensor operation at elevated temperature itself causes gradual changes in the tin oxide film properties, which in turn deviate gas sensing properties of the device with time (Hu et al. 2003, Kuang et al. 2007). Therefore, it is highly desirable to have sensors, which can operate at room temperature, but having comparable properties with that of tin oxide for gas sensing. Therefore further improvement in methods of material synthesis, surface modifications and sensor fabrication technologies, are required to achieve better performance in tin oxide based gas sensor (Xue et al. 2005, Zhang et al. 2008). Many pure and doped SnO_2 have been exposed with high sensing characteristics. Recently, many materials, such as Zn, Pt, Pd and Al have been proved to be effective dopants for the improvements of response or reaction speed or other characteristics of SnO_2 (Kolmakov et al. 2005). Al is often chosen because of its properties that improve the oxygen dissociation reaction and its ability to change its oxidation state easily according to the gas environment (Korotcenkov and Cho 2012). In the last few decades, nanofibers have attracted the attention of researchers due to their remarkable micro and nano structural characteristics, high surface area, small pore size, and the possibility of their producing three dimensional structures that enable the development of advanced materials with sophisticated applications. Nanofibers of aluminum (Al) doped SnO_2 showed improved sensing properties due to increase in the magnitude of conductivity, but the high operating temperature (280-450 ˚C) of these sensors may be inadequate for measuring high H_2 concentrations due to the danger of explosions. The conducting polymers have improved many aspects of the gas sensors especially in lowering the operating temperature to around room temperature. In addition to this, the ability to incorporate specific binding sites into conducting polymers promises the improvement of selectivity and sensitivity (Marsella et al. 1995). Among the various conducting polymers, Polyaniline (PANI) has been investigated as a potential material for H_2 gas sensing applications, due to its controllable electrical conductivity, environmental stability and interesting redox properties associated with the chain nitrogen's (Heeger 2002, MacDiarmid 2002). It is the unique type of conducting polymer in which the charge delocalization can, in principle, offer multiple active sites on its backbone for the adsorption and desorption of H_2 gas. Hybridization of metal oxide and conducting polymer could improve the properties of pure metal oxides or conducting polymers based gas sensor (Arora et al, 2014). Since, the Nanofibers of polymeric materials i.e. nanofibers of Al-SnO_2/PANI composites have large aspect ratio, large surface area to volume ratio and large porosity, such materials are best for sensing of different gases due to larger absorptive capacity for gas analyte.

The interest in developing solid-state hydrogen gas sensor is due to the fact that presently hydrogen is considered as 'near- future' fuel. However, as hydrogen is highly explosive, safety remains a top priority. Hydrogen gas leaks easily from gas lines and systems and is one of the most explosive gases. In fact, a number of problems arise involving the storage of this gas. For this reason, there is a big demand of reliable, flexible and inexpensive H_2 gas sensors to prevent accidents due to its leakage, thus, saving lives and infrastructure (Adamyan et al. 2007, Ramesh et al. 2004). Hydrogen gas sensors can quickly and reliably detect hydrogen over a wide range of oxygen and moisture concentrations are not currently available (Ramesh et al. 2004, Yamazaki et al. 2005). At present, commercial hydrogen detectors are not suitable for widespread use, particularly in transportation, because they are too bulky, expensive, and some are dangerous (Yan et al. 2009, Fawcett et al. 2004). From the standpoint of the safety with the global environment, it is necessary today to develop new hydrogen gas sensors working at or near room temperature by using polymeric material at nanolevel. In addition, they should be small, cheap and easy to be implanted into microelectronic IC (Aroutiounian 2007, Shukla et al. 2003). In this work, a high-efficiency hydrogen sensor based on Al-SnO_2/PANI composite nanofibers has been fabricated via electrospinning technique. Electrospinning seems to be the simplest and most versatile technique capable of generating (1D) nanostructures.

2. Experimental

2.1. Materials and Methods

$SnCl_2 \cdot 2H_2O$, Aniline monomer (distilled under reduced pressure), ammonium peroxydisulphate (APS) and Polyvinyl pyrrolidone (PVP, Mw=1,300,000) were purchased from Aldrich. All supplement chemicals were of AR grade and used as received.

2.2. Fabrication of Al-SnO_2 / PANI composite nanofibers

In a typical procedure, 0.4 g of $SnCl_2 \cdot 2H_2O$ was dissolved in 0.4 g of as-prepared PANI/CSA from chemical oxidative method. Then, 4.4 g of DMF and 4.4 g of ethanol were mixed in it under vigorous stirring for 30 min. Subsequently, 1% Al $(NO_3)_3.9H_2O$ and 1.0 g PVP were added into the above solution under vigorous stirring for 45 min. The mixture was loaded into a glass syringe with a needle of 0.5mm in diameter at the tip and was electrified using a high-voltage DC supply. Calcination (400˚C in air for 5 h) was performed to remove the organic constituents of PVP and crystallize the Al-SnO_2. For electrospinning, the solution was kept in a vertical syringe with a stainless steel needle having an orifice of 0.5mm. The needle was electrically connected to a positive high voltage. 17 kV was provided between the tip of the spinning nozzle and the collector at a distance of 20 cm and the solution flow rate was kept at 0.4 ml/h, maintained using computer control programmer. Fig. 1 shows the systematic illustration of the whole process of synthesis of nanofibers for hydrogen sensing. The as-prepared nanofibers were characterized by Scanning electron microscopy (SEM, Carl Zeiss Model EVO-18, JSM-7600F), X-ray Diffraction (XRD, PANalytical diffractometer with Cu Kα), UV-Visible spectroscopy (SHIMADZU Spectrophotometer, Model-UV-1800), Fourier transform infrared spectroscopy (FTIR, Bruker Alpha Spectrophotometer) and Hydrogen gas sensing (Keitheley instruments Inc-Model 2000).

3. Results and discussion

3.1. Scanning Electron Microscopy (SEM)

Fig. 2 (a) and 2 (b) shows the typical SEM images of 1% Al-SnO_2 and 1 % Al-SnO_2/PANI nanofibers respectively. From SEM micrographs, it is revealed that diameter of as-synthesized 1% Al-SnO_2/PANI nanofibers increased as compared to pristine Al-SnO_2 having the diameter of 200 nm may be due to encapsulation of PANI on the surface of Al-SnO_2 composite, Kondawar et al. (2011). Morphologically, nanofibers of Al-SnO_2 are uniform and fibers of Al-SnO_2/PANI are not, which may be due to change in viscosity and surface tension of the solution prepared using equimass of PANI and $SnCl_2.2H_2O$. While comparing the porosity from their SEM images, Al-SnO_2/PANI shows more porous structure than that of the pristine Al-SnO_2 nanofibers which causes better sensing properties even at low operating temperature.

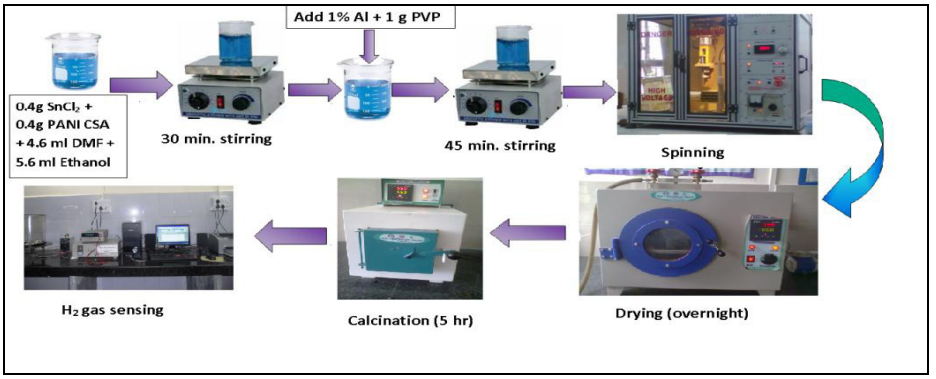

Fig. 1: Schematic illustration of the processes involved to prepare nanofibers for H_2 Sensing

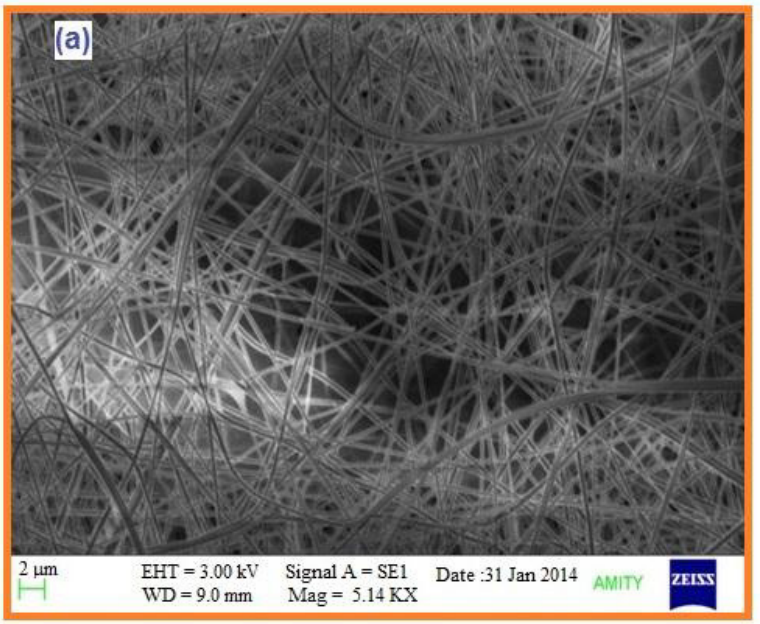

Fig. 2(a): SEM image of 1% Al-SnO_2 nanofibers

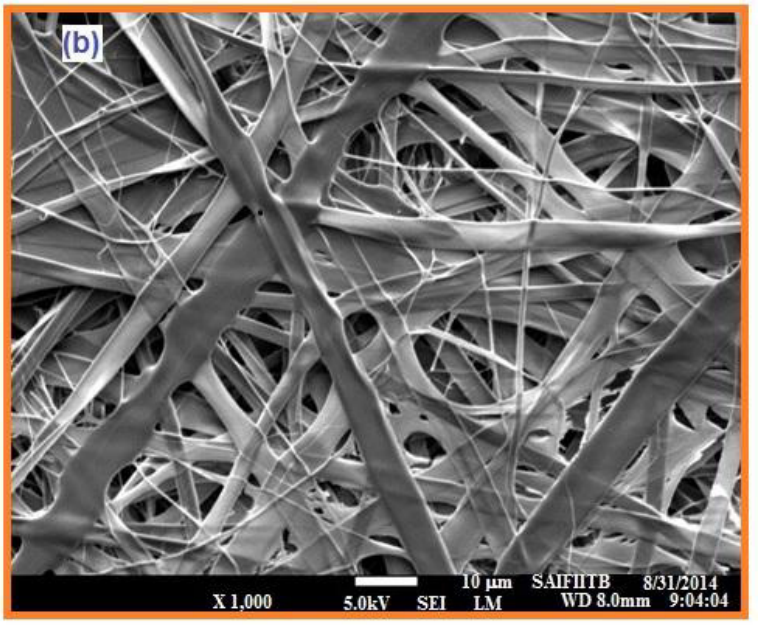

Fig. 2(b) SEM image of 1% Al-SnO_2/PANI nanofibers

3.2. UV-VIS spectroscopy

UV-VIS spectroscopy was utilized to understand the electronic states of Al-SnO_2 and Al-SnO_2/PANI. Fig. 3(a) shows UV-VIS spectra of 1% Al-SnO_2 and 1% Al-SnO_2/PANI nanofibers. The 1% Al-SnO_2/PANI showed two characteristic bands, one at 404 nm in visible region corresponds to inter ring charge transfer ratio of benzenoid to quinoid moieties showing polaron-π^* transition and arises owing to the doping level and the formation of polarons,

MacDiarmid and Epstein (1994) or Jiang et al. (1997) or Kim et al. (2001) and other at 324 nm in UV corresponds to π-π* transition of benzenoid ring and the insertion of Al-SnO_2 in PANI. Optical absorbance studies for 1% Al-SnO_2 also shows the exact value 324 nm of characteristic peak due to the presence of Al-SnO_2 in PANI matrix.

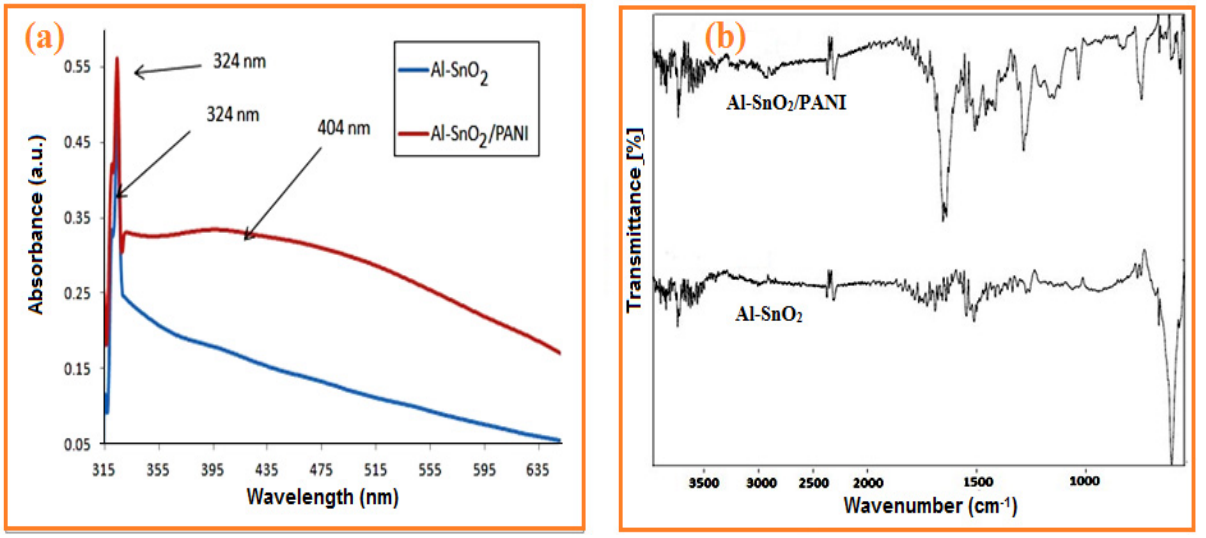

Fig. 3. (a) UV-VIS spectra and (b) FTIR spectra of 1% Al-SnO_2 and 1% Al-SnO_2 /PANI nanofibers

3.3. Fourier Transform Infrared Spectroscopy (FTIR)

The FTIR spectra of Al-SnO_2 and Al-SnO_2/PANI nanofibers are shown in Fig. 3(b). Al-SnO_2/PANI nanofibers shows the peak at 3743 cm^{-1} associated with the interaction between Al-SnO_2 and PANI by formation of hydrogen bonding between H-N and oxygen of SnO_2. The vibration band seen around 2376 cm^{-1} has been ascribing to the aromatic C-H vibration. The 1550-1650 cm^{-1} vibration band is due to the C-N stretching vibration of quinoid rings whereas 1439-1498 cm^{-1} vibration band arises due to the C-N stretching vibration associated with the benzenoid ring of PANI. In the region close to 1350 cm^{-1} the peaks are attributed to the presence of aromatic amines present in polyaniline. The 1038 cm^{-1} vibration band is due to S=O bonding for camphor sulphonic acid and the peaks at around 650-750 cm^{-1} corresponds to the C-C, C-H bonding mode of aromatic ring and which is due to the Sn-O-Sn stretching. Al-SnO_2 nanofibers shows a broad peak around 600 nm corresponds to the Sn-O-Sn stretching which confirms the formation of Al-SnO_2.

3.4. X-Ray Diffraction

Fig. 4 shows the XRD patterns for 1% Al-SnO_2 and 1% Al-SnO_2/PANI nanofibers. All the strong diffraction peaks of Al-SnO_2 nanofibers can be perfectly indexed as the tetragonal rutile structure for SnO_2 (ICDD DATA CARD 41-1445), Chang et al. (2008). There is no indication of the presence of any dopants-related diffraction peaks for the Al-doped sample implying the high dispersion or the poor crystallinity of dopant related nanoparticles. In the Al-SnO_2/PANI nanofibers, most of the peaks are found to be broadened due the polycrystalline effect of PANI as compared to those of Al-SnO_2. The broad peak due to PANI around 26˚ has been found to be merged with that of Al-SnO_2 at 26.66˚. In addition, the reduced intensity of the peaks was observed compared with the XRD of pure Al-SnO_2. The main dominant peaks of Al-SnO_2 were identified at 2θ = 26.66˚, 34.18˚, 52.3˚, 61.34˚, 64.4˚ and 65.54˚ which corresponding to (1 1 0), (1 0 1), (2 1 1), (1 1 2), (3 0 1) and (3 0 2) and the three

strong peaks are assigned to the (1 1 0), (1 0 1) and (2 1 1). PANI deposited on the surface of Al-SnO_2 particles has no effect on the crystallization behaviour of Al-SnO_2 particles in the nanocomposites.

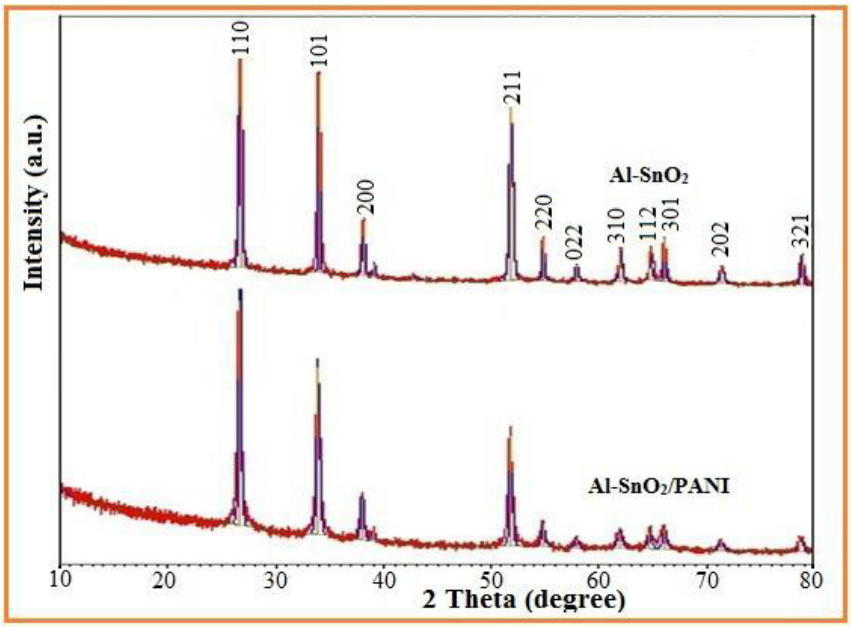

Fig. 4. XRD patterns of 1% Al-SnO_2 and 1% Al-SnO_2/PANI nanofibers

3.5. Hydrogen Gas Sensing

In order to systematically investigate the hydrogen gas sensing properties of 1% Al-SnO_2/PANI nanofibers sensor in comparison with the 1% Al-SnO_2, the study of gas sensing response for 1000 ppm with temperature was carried out. A series of experiments at different temperatures was performed to obtain the optimal operating temperature for H_2 detection. Before exposing to the target gas, sensor was stabilized for 6 hour at the room temperature and then the temperature was computerized set when the sensor was exposed to 1000 ppm of hydrogen gas with help of (Keitheley instruments Inc. Model 2000). Fig. 5 (a) and Fig. 5 (b) represents the sensitivity and response to H_2 gas respectively for the 1% Al-SnO_2/PANI nanofibers.

It has been observed that there is no appreciable change in the resistance of 1% Al-SnO_2, on exposure to different concentrations of H_2 gas at room temperature. It was found that 1% Al-SnO_2/PANI nanofibers showed better response to H_2 gas as compared to that of 1% Al-SnO_2 reported, Xu et al. (2011). The maximum sensitivity at very low temperature (48 ^{o}C) was observed for 1% Al-SnO_2/PANI nanofibers, whereas 1% Al-SnO_2 nanofibers showed the maximum sensitivity at 340˚C for 100 ppm hydrogen gas, Xu et al. (2011). When PANI mixed with Al-SnO_2, then nanocomposite will have synergistic effect of both the components due to which the composite material requires less amount of energy for the electrons to move from valance band to conduction band i.e. the carrier mobility increases. In presence of Al-SnO_2 crystallites, the PANI matrix gets modified structure electronically. Therefore, the resulting material will operate at lower temperatures compared to pure Al-SnO_2. On exposure to H_2 gas, 1% Al-SnO_2/PANI nanofibers film resistance decreased by more than an order of magnitude from its original value, indicating that the electrical resistance of the film is a sensitive parameter in the presence of hydrogen gas. Al-SnO_2 crystallites being an n-type surrounded by p-type PANI molecules make p–n junction like formation locally in composite film. The n-type nature of Al-SnO_2 crystallites annihilate the holes of PANI molecules, near its

boundary making a depletion region, which in turn makes the overall PANI matrix electrically more insulating in nature, Deshpande et al. (2009). On exposing the composite film with hydrogen which can be permeated into the PANI matrix freely, some of the hydrogen molecules might reach into the depletion region, which is surrounding the Al-SnO_2 crystallite and act as a dielectric between the PANI and Al-SnO_2 border. The depletion region field might polarize the hydrogen molecules, and in turn provide a positive charge to PANI molecules, which can become mobile on its transfer to the central N atom of PANI molecule. This process creates some free holes on PANI molecules, which increase the hopping conductivity of the film, and therefore make the composite film relatively more conducting electrically. Once the process of polarizing the hydrogen molecules by p–n junction like formation is saturated, this mechanism cannot generate additional holes in the composite PANI film and therefore no additional change in the film conductivity occurs even by further addition of hydrogen to it.

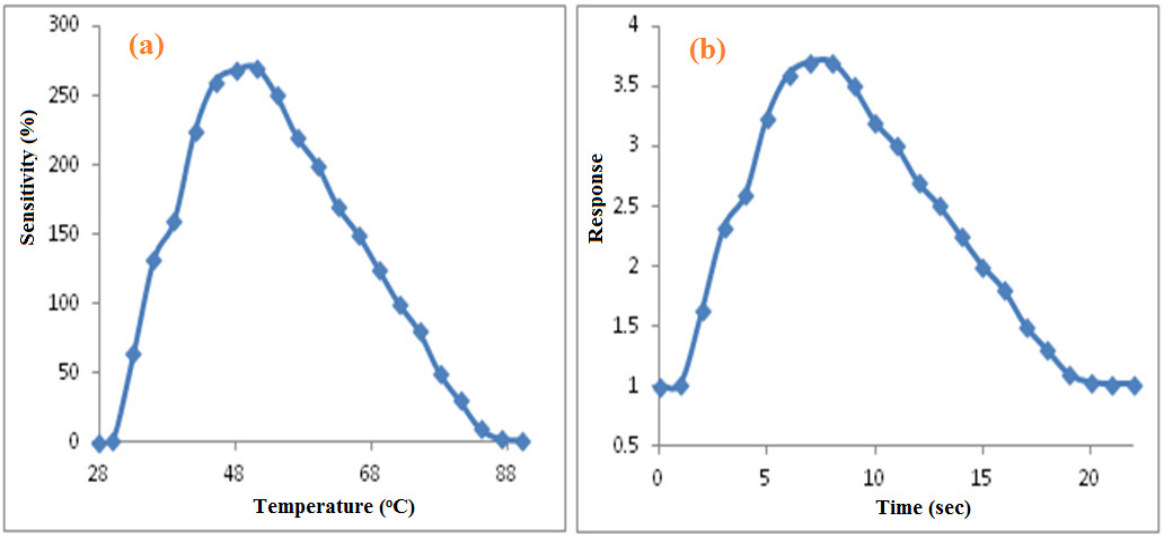

Fig. 5 (a) Sensitivity and (b) Response of 1% Al-SnO_2/PANI nanofibers

The response of sensor was monitored in terms of the normalized resistance calculated by Response = R_0/Rg and the sensitivity factor was monitored in terms of the % sensitivity calculated by % sensitivity = $\Delta R/R_0$. Where ΔR is the variation in resistance of composite films from baseline after exposure to H_2 gas, Rg is the resistance of the sensor in presence of H_2 gas and R_0 is the initial baseline resistance of the films and as per the definitions of 'Response time (R_P)' and 'Recovery time (R_C)' for gas sensing, the values of R_P and R_C for 1% Al-SnO_2/PANI nanofibers were estimated to be ~2 sec and ~ 2 sec respectively while 'Response time (R_P)' and 'Recovery time (R_C)' for 1% Al-SnO_2 were estimated to be ~3 sec and ~ 2 sec respectively at 340˚C for 100 ppm hydrogen gas.

4. Conclusion

The nanofibers of Al-SnO_2 and Al-SnO_2/PANI composite with the diameter around 200-300 nm were synthesized successfully via electrospinning technique. The interaction between aluminum doped SnO_2 and PANI was confirmed from FTIR, UV-VIS and XRD spectra. The 1% Al-SnO_2/PANI hybrid material showed high sensitivity to H_2 gas (1000ppm) at an operated temperature 48˚C with relatively faster response and recovery. In comparison to the pure SnO_2, Al-SnO_2 and PANI based sensors reported earlier, the 1% Al-SnO_2/PANI sensor in the present study exhibits the faster response and higher sensitivity for hydrogen gas at room temperature.

Acknowledgement

The authors acknowledge Department of Science & Technology, New Delhi (India) for financial assistance under; INSPIRE Fellowship 2013. Sanction Order No. & Date: DST/INSPIRE Fellowship/2013/92, dated 17th May 2013. Registration No: [IF130149]

References

Adamyan, A.Z., Adamyan, Z.N., Aroutiounian, V.M., Arakelyan, A.H., Touryan, K.J., Turner, J.A., 2007. Sol–gel derived thin film semiconductor hydrogen gas sensor. International Journal of Hydrogen Energy 32, 4101-4108.

Arora, R., Mandal, U., Sharma, P., Srivastav, A. 2014. Effect of fabrication technique on microstructure and electrical conductivity of polyaniline-TiO_2-PVA composite material. Procedia Materials Science 6, 238–243.

Aroutiounian, V., 2007. Metal oxide hydrogen, oxygen, and carbon monoxide sensors for hydrogen setups and cells. International Journal of Hydrogen Energy 32, 1145-1158.

Berry, L., Brunet, J., 2008. Oxygen influence on the interaction mechanisms of ozone on SnO_2 sensors. Sensors and Actuators B: Chemical 129, 450-458.

Binions, R., Naik, A.J.T., 2013. 13 – Metal oxide semiconductor gas sensors in environmental monitoring. Semiconductor Gas Sensors, A volume in Woodhead Publishing Series in Electronic and Optical Materials, 433-466.

Chang, S.J., Hsueh, T.J., Chen, I.C., Hsieh, S.F., Chang, S.P., Hsu, C.L., Lin, Y.R., Huang, B.R., 2008. Highly sensitive ZnO nanowire acetone vapor sensor with Au adsorption. IEEE Transactions on Nanotechnology 7, 754-759.

Deshpande, N.G., Gudage, Y.G., Sharma, R., Vyas, J.C., Kim, J.B., Lee, Y.P., 2009. Studies on tin oxide-intercalated polyaniline nanocomposite for ammonia gas sensing applications. Sensors and Actuators B 138, 76-84.

Fawcett, T.J., Wolan, J.T., Myers, R.L., Walker, J., Saddow, S.E., 2004. Wide-range (0.33–100%) 3C–SiC resistive hydrogen gas sensor development. Applied Physics Letters 85, 416-418.

Heeger, A.J., 2002. Semiconducting and metallic polymers: the fourth generation of polymeric materials. Synthetic Metals 125, 23-42.

Hieu, N.V., Kim, H.R., Ju, B.K., Lee, J.H., 2008. Enhanced performance of SnO_2 nanowires ethanol sensor by functionalizing with La_2O_3. Sensors and Actuators B: Chemical 133, 228-234.

Hu, J., Bando, Y., Liu, Q., Golberg, D., 2003. Laser-ablation growth and optical properties of wide and long single-crystal SnO_2 ribbons. Advanced Functional Materials 13, 493-496.

Hyodo, T., Baba, T.Y., Wada, K., Shimizu, Y., Egashira, M., 2000. Hydrogen sensing properties of SnO_2 varistors loaded with SiO_2 by surface chemical modification with diethoxydimethylsilane. Sensors and Actuators B 64, 175-81.

Jiang, H., Geng, Y., Li, J., Wang, F., 1997. Organic acid doped polyaniline derivatives. Synthetic Metals 84, 125-126.

Kim, B.J., Oh, S.G., Han, M.G., Im, S.S, 2001. Synthesis and characterization of polyaniline nanoparticles in SDS micellar solutions. Synthetic Metals 122, 297-304.

Kolmakov, A., Klenov, D.O., Lilach, Y., Stemmer, S., Moskovits, M., 2005. Enhanced gas sensing by individual SnO_2 nanowires and nanobelts functionalized with Pd catalyst particles. Nano Letters 5, 667-673.

Kondawar, S.B., Acharya, S.A., Dhakate, S.R., 2011. Microwave assisted hydrothermally synthesized nanostructure zinc oxide reinforced polyaniline nanocomposites. Advanced Materials Letters 2, 362-367.

Korotcenkov, G., Cho B.K., 2012. Ozone measuring: What can limit applications of SnO_2- based Conductometric gas sensors? Sensors and Actuators B: Chemical 161, 28-44.

Kuang, Q., Lao, C., Wang, Z.L., Xie, Z., Zheng, L., 2007. High-sensitivity humidity sensor based on a single SnO_2 nanowire. Journal of American Chemical Society 129, 6070-6071.

MacDiarmid, A.G., 2002. A novel role for organic polymers. Synthetic Metals 125, 11-22.

MacDiarmid, A.G., Epstein, A.J., 1994. The concept of secondary doping as applied to polyaniline. Synthetic Metals 65, 103-116.

Marsella, M.J., Carroll, P.J., Swager, T.M., 1995. Conducting pseudopolyrotaxanes: a chemoresistive response via molecular recognition. Journal of American Chemical Society 116, 9347-8.

Patil, L.A., Pathan, I.G., Suryawanshi, D.N., Bari, A.R., Rane, D.S., 2014. Spray pyrolyzed $ZnSnO_3$ nanostructure thin films for hydrogen sensing. Procedia Materials Science 6, 1557–1565.

Qiu, J., Zhang, S., Zhao, H., 2011. Recent applications of TiO_2 nanomaterials in chemical sensing in aqueous media. Sensors and Actuators B 160, 875- 890.

Ramesh, C., Velayutham, G., Murugesan, N., Ganesan, V., Manivannan, V., Periaswami, G., 2004. Studies on modified anode polymer hydrogen sensor. Ionics 10, 50-55.

Shukla, S., Patil, S., Kuiry, S.C., Rahman, Z., Du, T., Ludwig, L., Parish, C., Seal, S., 2003. Synthesis and Characterization of sol-gel derived nanocrystalline tin oxide thin film as hydrogen sensor. Sensors and Actuators B 96, 343-353.

Tai, H., Jiang, Y., Xie, G., Yu, J., Chen, X., 2007. Fabrication and gas sensitivity of polyaniline–titanium dioxide nanocomposite thin film. Sensors and Actuators B 125, 644-650.

Tischner, A., Maier, T., Stepper, C., Kock, A., 2008. Ultrathin SnO_2 gas sensors fabricated by spray pyrrolysis for the detection of humidity and carbon monoxide. Sensors and Actuators B: Chemical 134, 796-802.

Xue, X.Y., Chen, Y.J., Wang, Y.G., Wang, T.H., 2005. Synthesis and ethanol sensing properties of $ZnSnO_3$ nanowires. Applied Physics Letters 86, 233101/1-1233101/.

Xu, X., Sun, J., Zhang, H., Wang, Z., Dong, B., Jiang, T., Wang, W., Li, Z., Wang, C., 2011. Effects of Al doping on SnO_2 nanofibers in hydrogen sensor. Sensors and Actuators B 160, 858-863.

Yamazaki, T., Okumura, H., Jin, C. Ji, Nakayama, A., Kikuta, T., Nakatani, N., 2005. Effect of density and thickness on H_2-gas sensing property of sputtered SnO_2 films. Vacuum 77, 237-243.

Yan, Q., Tao, S., Toghiani, H., 2009. Optical fiber evanescent wave absorption spectrometry of nanocrystalline tin oxide thin films for selective hydrogen sensing in high temperature gas samples. Talanta 77, 953-961.

Zhang, Y., He, X., Li, J., Miao, Z., Huang, F., 2008. Fabrication and ethanol-sensing properties of micro gas sensor based on electrospun SnO_2 nanofibers. Sensors and Actuators B: Chemical 132, 67-73.